

Partonic effects on higher-order anisotropic flows in relativistic heavy-ion collisions

Lie-Wen Chen,^{1,*} C. M. Ko,¹ and Zi-Wei Lin²

¹*Cyclotron Institute and Physics Department, Texas A&M University, College Station, Texas 77843-3366*

²*Physics Department, Ohio State University, Columbus, Ohio 43210*

(Dated: June 22, 2020)

Higher-order anisotropic flows v_4 and v_6 in heavy ion collisions at the Relativistic Heavy Ion Collider are studied in a multiphase transport model that has previously been used successfully for describing the elliptic flow v_2 in these collisions. We find that the same parton scattering cross section of about 10 mb used in explaining the measured v_2 can also reproduce the recent data on v_4 and v_6 from Au + Au collisions at $\sqrt{s} = 200$ AGeV. It is further found that the v_4 is a more sensitive probe of the initial partonic dynamics in these collisions than v_2 . Moreover, higher-order parton anisotropic flows are nonnegligible and satisfy the scaling relation $v_{n,q}(p_T) \sim v_{2,q}^{n/2}(p_T)$, which leads naturally to the observed similar scaling relation among hadron anisotropic flows when the coalescence model is used to describe hadron production from the partonic matter.

PACS numbers: 25.75.Ld, 24.10.Lx

I. INTRODUCTION

There have been extensive studies on the azimuthal anisotropy of hadron momentum distributions in the transverse plane perpendicular to the beam direction, particularly the lower-order elliptic flow v_2 , in heavy ion collisions at various energies [1]. The hadron transverse momentum anisotropy is generated from the pressure anisotropy in the initial compressed matter formed in non-central heavy ion collisions [2, 3] and is thus sensitive to the properties of the produced matter. This sensitivity not only exists in the larger elliptic flow [4, 5, 6, 7, 8, 9] but also in the smaller higher-order anisotropic flows [10, 11, 12]. Recently, higher-order anisotropic flows v_4 , v_6 , and v_8 in heavy ion collisions at the Relativistic Heavy Ion Collider (RHIC) were studied in more detail using the hydrodynamical model [13], and it was suggested that the v_4 could also provide important information on the collision dynamics during the early stage. Although the hadron anisotropic flows become smaller with increasing orders, recent experimental results from the STAR Collaboration [14] have demonstrated that they are still measurable.

In the present work, the anisotropic flows v_2 , v_4 , and v_6 of both partons and hadrons in heavy ion collisions at RHIC are studied in a multiphase transport (AMPT) model that includes initial partonic and final hadronic interactions [15, 16]. Using the version with string melting, i.e., allowing hadrons that are expected to be formed from initial strings to convert to their valence quarks and anti-quarks [17, 18, 19], we find that the measured data from Au + Au collisions at $\sqrt{s} = 200$ AGeV can be approximately reproduced if a parton scattering cross section of about 10 mb is used in the model. Our results show that the hadron v_4 is indeed a more sensitive probe of the

initial partonic dynamics in relativistic heavy ion collisions than the v_2 . We also find that higher-order parton anisotropic flows are nonnegligible and satisfy the scaling relation $v_{n,q}(p_T) \sim v_{2,q}^{n/2}(p_T)$, which then leads to a similar scaling relation among hadron anisotropic flows if hadron production from the partonic matter can be described by the quark coalescence model.

II. THE AMPT MODEL

The AMPT model is a hybrid model that uses minijet partons from hard processes and strings from soft processes in the HIJING model [20] as the initial conditions for modeling heavy ion collisions at ultra-relativistic energies. Time evolution of resulting minijet partons is then described by the ZPC [21] parton cascade model. At present, this model includes only parton-parton elastic scatterings with an in-medium cross section given by:

$$\frac{d\sigma_p}{dt} = \frac{9\pi\alpha_s^2}{2} \left(1 + \frac{\mu^2}{s}\right) \frac{1}{(t - \mu^2)^2}, \quad (1)$$

where the strong coupling constant α_s is taken to be 0.47, and s and t are the usual Mandelstam variables. The effective screening mass μ depends on the temperature and density of the partonic matter but is taken as a parameter in ZPC for fixing the magnitude and angular distribution of parton scattering cross section. After minijet partons stop interacting, they are combined with their parent strings, as in the HIJING model with jet quenching, to fragment into hadrons using the Lund string fragmentation model as implemented in the PYTHIA program [22]. The final-state hadronic scatterings are then modeled by the ART model [23].

The default AMPT model [15] has been quite successful in describing measured rapidity distributions of charge particles, particle to antiparticle ratios, and spectra of low transverse momentum pions and kaons [16] in heavy ion collisions at the Super Proton Synchrotron

*On leave from Department of Physics, Shanghai Jiao Tong University, Shanghai 200030, China

(SPS) and RHIC. It has also been useful in understanding the production of J/ψ [24] and multistrange baryons [25] in these collisions. Since the initial energy density in Au + Au collisions at RHIC is much larger than the critical energy density at which the hadronic matter to quark-gluon plasma transition would occur [24, 26], the AMPT model has been extended to convert the initial excited strings into partons [17]. In this string melting scenario, hadrons, that would have been produced from string fragmentation, are converted instead to valence quarks and/or antiquarks. Interactions among these partons are again described by the ZPC parton cascade model. The transition of the partonic matter to the hadronic matter is, however, achieved using a simple coalescence model, which combines two nearest quark and antiquark into mesons and three nearest quarks or antiquarks into baryons or anti-baryons that are close to the invariant mass of these partons. Using parton scattering cross sections of 6-10 mb, the extended AMPT model is able to reproduce both the centrality and transverse momentum (below 2 GeV/c) dependence of the elliptic flow [17] and pion interferometry [18] measured in Au+Au collisions at $\sqrt{s} = 130$ AGeV at RHIC [27, 28]. It has also been used for studying the kaon interferometry in these collisions [29]. This latter version of the AMPT model with string melting is used in the following to study hadron anisotropic flows in heavy ion collisions at RHIC.

III. ANISOTROPIC FLOWS

Hadron anisotropic flows v_n are the Fourier coefficients in the decomposition of their transverse momentum spectra in the azimuthal angle ϕ with respect to the reaction plane [30], i.e.,

$$E \frac{d^3 N}{dp^3} = \frac{1}{2\pi} \frac{dN}{p_T dp_T dy} [1 + \sum_{n=1}^{\infty} 2v_n(p_T, y) \cos(n\phi)] \quad (2)$$

Because of the symmetry $\phi \leftrightarrow -\phi$ in the collision geometry, no sine terms appear in the above expansion. For hadrons at midrapidity in collisions with equal mass nuclei, which will be considered in the present study, anisotropic flows of odd orders vanish as a result of the symmetry $\phi \leftrightarrow \phi + \pi$. The anisotropic flows generally depend on the particle transverse momentum and rapidity, and for a given rapidity the anisotropic flows at transverse momentum p_T can be evaluated from

$$v_n(p_T) = \langle \cos(n\phi) \rangle, \quad (3)$$

where $\langle \dots \rangle$ denotes average over the azimuthal distribution of particles with transverse momentum p_T . The anisotropic flows v_n can further be expressed in terms of following single-particle averages:

$$v_2(p_T) = \left\langle \frac{p_x^2 - p_y^2}{p_T^2} \right\rangle \quad (4)$$

$$v_4(p_T) = \left\langle \frac{p_x^4 - 6p_x^2p_y^2 + p_y^4}{p_T^4} \right\rangle \quad (5)$$

$$v_6(p_T) = \left\langle \frac{p_x^6 - 15p_x^4p_y^2 + 15p_x^2p_y^4 - p_y^6}{p_T^6} \right\rangle \quad (6)$$

$$v_8(p_T) = \left\langle \frac{p_x^8 - 28p_x^6p_y^2 + 70p_x^4p_y^4 - 28p_x^2p_y^6 + p_y^8}{p_T^8} \right\rangle \quad (7)$$

where p_x and p_y are, respectively, projections of particle momentum in and perpendicular to the reaction plane.

Since the AMPT model also provides information on the spatial anisotropy of colliding matter, which is responsible for generating the momentum anisotropic flows, it is of interest to introduce the spatial anisotropic coefficient s_n by expressions similar to those for the anisotropic flows v_n but in terms of the spatial distributions of particles in the transverse plane.

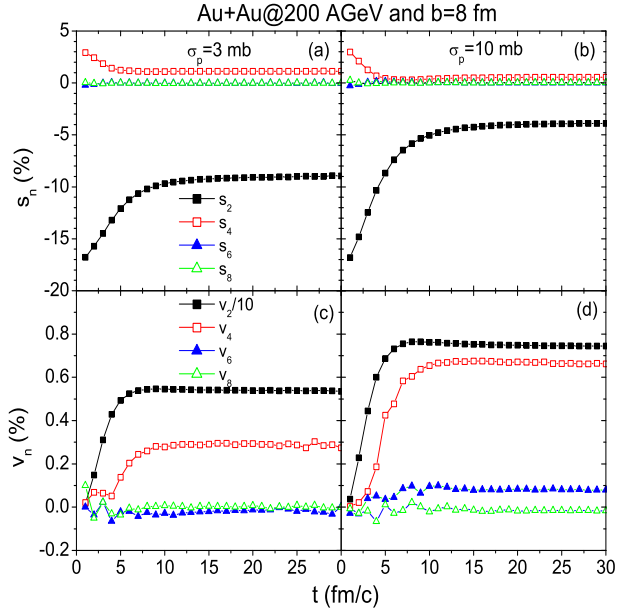


FIG. 1: (Color online) Time evolutions of spatial anisotropic coefficients s_n and anisotropic flows v_n of partons in midrapidity from Au + Au collisions at $\sqrt{s} = 200$ AGeV and $b = 8$ fm for parton scattering cross sections $\sigma_p = 3$ mb (left panels) and $\sigma_p = 10$ mb (right panels).

Using the AMPT model in the string melting scenario with parton scattering cross sections $\sigma_p = 3$ and 10 mb, we have studied the time evolutions of s_n and v_n of partons in the midrapidity from Au + Au collisions at $\sqrt{s} = 200$ AGeV and $b = 8$ fm, and they are shown in Fig. 1. The spatial anisotropic coefficients s_n at a given time are evaluated using parton positions at their last interactions before this time as in Ref.[17]. In this way, final values of s_n are given by the parton spatial distributions at freeze out. Similarly, final values of v_n are determined by the parton momentum distributions at freeze out, when they are converted to hadrons in the

AMPT model by coalescence. It is seen from Figs. 1(a) and (b) that the spatial elliptic deformation s_2 is initially large and decreases with time. It reaches the saturation value at about $10\text{-}15 \text{ fm}/c$ for both parton scattering cross sections. The same behavior is observed for the fourth-order spatial anisotropic coefficient s_4 except that it reaches the saturation value earlier at about $5 \text{ fm}/c$. The higher-order spatial anisotropic coefficients s_6 and s_8 are essentially zero. The nonzero spatial anisotropic coefficients s_n imply that the parton spatial distribution is nonspherical at freeze out. We note that the larger parton scattering cross section leads to a smaller spatial anisotropy at freeze out.

The time evolutions of the momentum anisotropic flows v_n are shown in Figs. 1(c) and (d) for the two parton scattering cross sections of 3 and 10 mb, respectively. The elliptic flow v_2 is seen to saturate earlier in the collisions, i.e., at about $7 \text{ fm}/c$. This is similar for both parton scattering cross sections, except that the larger one leads to a larger elliptic flow. As to v_4 , its value reaches its final value at a later time than that for v_2 , i.e., at about $10 \text{ fm}/c$, which may be due to the fact that the parton v_2 also affects its v_4 . For other higher-order momentum anisotropic coefficients, the v_6 is very small, having a magnitude less than 0.1% for both parton scattering cross sections, while v_8 is essentially zero. An interesting result predicted by the AMPT model is that the v_4 is more sensitive to the parton cross section than the v_2 . For instance, the final values of v_2 and v_4 are about 5.4% and 0.29%, respectively, for $\sigma_p = 3 \text{ mb}$, and they are increased to about 7.5% and 0.67%, respectively, for $\sigma_p = 10 \text{ mb}$. Therefore, the v_4 is enhanced by a factor of about 2.3 while the v_2 is only enhanced by a factor of about 1.4, when the parton cross section is increased by a factor of about 3.

The anisotropic flows of partons are transferred to those of hadrons when the latter are formed from the coalescence of quarks and/or antiquarks. Because of the small spatial anisotropy and pressure in the resulting hadronic matter, the hadron anisotropic flows remain essentially unchanged during subsequent evolution [17]. In Fig. 2, we show the final anisotropic flows v_n of all charged hadrons in the pseudorapidity range $|\eta| < 1.2$ in minimum bias Au + Au collisions at $\sqrt{s} = 200 \text{ AGeV}$ as functions of transverse momentum p_T for parton scattering cross sections $\sigma_p = 3$ and 10 mb. Also included in Fig. 2 are recent experimental data from the STAR collaboration [14]. It is seen that the parton scattering cross section $\sigma_p = 3 \text{ mb}$ underestimates the data at higher p_T ($> 1 \text{ GeV}/c$) while $\sigma_p = 10 \text{ mb}$ seems to give a better fit to the data. The values of v_6 are in agreement with the data within error bars, although they are essentially zero. Again, the v_4 exhibits a stronger sensitivity to the parton cross section than the v_2 , especially at higher p_T . Therefore, the v_4 provides a more sensitive probe of the initial partonic dynamics in relativistic heavy ion collisions than the v_2 .

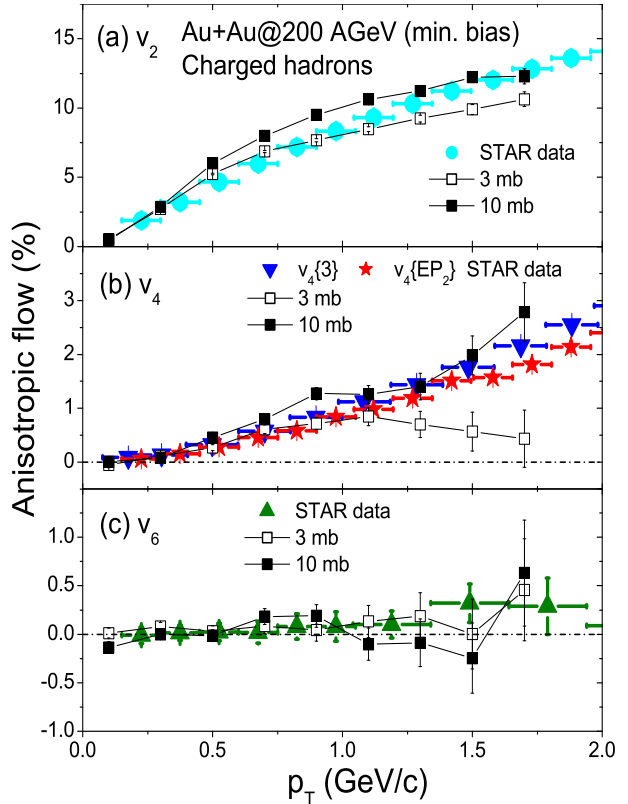


FIG. 2: (Color online) Anisotropic flows v_2 (a), v_4 (b), and v_6 (c) of all charged hadrons in the pseudorapidity range $|\eta| < 1.2$ from minimum bias Au + Au collisions at $\sqrt{s} = 200 \text{ AGeV}$ as functions of transverse momentum p_T for parton scattering cross sections $\sigma_p = 3$ (open squares) and 10 (solid squares) mb. The experimental data are from the STAR Collaboration [14].

IV. SCALINGS IN ANISOTROPIC FLOWS

The experimental data indicate that there is a scaling relation among hadron anisotropic flows, i.e., $v_n(p_T) \sim v_2^{n/2}(p_T)$ [14]. It has been shown by Kolb [31] that such scaling relation follows naturally from a naive quark coalescence model [32] that only allows quarks with equal momentum to form a hadron. Assuming that quarks have no higher-order anisotropic flows, he found $v_{4,M}(p_T) = (1/4)v_{2,M}^2(p_T)$ for the anisotropic flows of mesons that dominate the yield of charged particles. The smaller scaling factor of 1/4 than the empirical value of about 1 indicates that higher-order quark anisotropic flows cannot be neglected. Including the latter contribution, one can show that

$$\frac{v_{4,M}(2p_T)}{v_{2,M}^2(2p_T)} \approx \frac{1}{4} + \frac{1}{2} \frac{v_{4,q}(p_T)}{v_{2,q}^2(p_T)}, \quad (8)$$

$$\frac{v_{6,M}(2p_T)}{v_{2,M}^3(2p_T)} \approx \frac{1}{4} \left(\frac{v_{4,q}(p_T)}{v_{2,q}^2(p_T)} + \frac{v_{6,q}(p_T)}{v_{2,q}^3(p_T)} \right). \quad (9)$$

The meson anisotropic flows thus satisfy the scaling relations if the quark anisotropic flows also satisfy such relations.

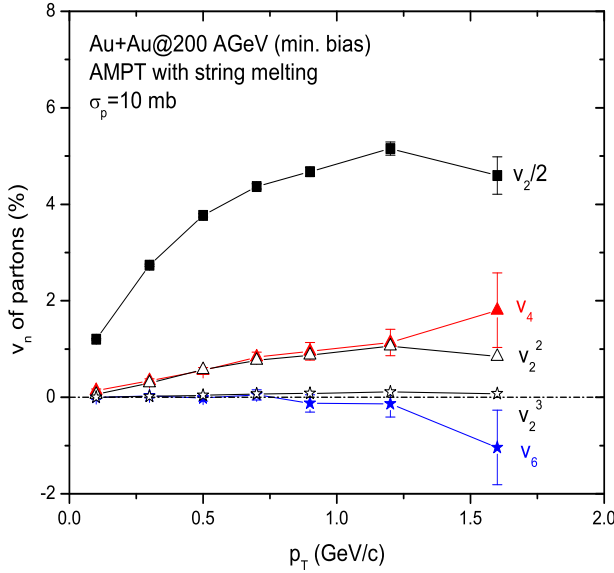


FIG. 3: (Color online) Transverse momentum dependence of midrapidity parton anisotropic flows v_2 , v_4 and v_6 from minimum bias events for Au + Au at $\sqrt{s} = 200$ AGeV with parton scattering cross section 10 mb. Also plotted are v_2^2 (open triangles) and v_2^3 (open stars).

In Fig. 3, we show the p_T dependence of the anisotropic flows v_2 , v_4 and v_6 of midrapidity partons from minimum bias events in Au + Au collisions at $\sqrt{s} = 200$ AGeV for a parton scattering cross section of 10 mb. Also shown in Fig. 3 are v_2^2 (open triangles) and v_2^3 (open stars). It is seen that the parton anisotropic flows from the AMPT transport model indeed satisfy the scaling relation $v_{n,q}(p_T) \sim v_{2,q}^{n/2}(p_T)$. With a parton scaling factor of about 1, we obtain the following scaling relations among meson anisotropic flows:

$$\frac{v_{4,M}(p_T)}{v_{2,M}^2(p_T)} \approx \frac{3}{4}, \quad \frac{v_{6,M}(p_T)}{v_{2,M}^3(p_T)} \approx \frac{1}{2}. \quad (10)$$

The resulting hadron scaling factors of 3/4 and 1/2 are, however, smaller than the one extracted from measured

anisotropic flows of all hadrons. Since the naive quark coalescence model does not allow hadron formation from quarks with different momenta as in more realistic quark coalescence models [33, 34, 35, 36], it is not expected to give a quantitative description of the experimental observation. Such effects are, nevertheless, included in the AMPT model, which have been shown in Fig. 2 to reproduce the measured hadron anisotropic flows.

V. SUMMARY

In summary, using a multiphase transport (AMPT) model in the string melting scenario, we have studied the anisotropic flows v_2 , v_4 , and v_6 of both partons and hadrons in heavy ion collisions at RHIC. We find that the anisotropic flows are developed early in the collision when the matter is in the partonic stage and has appreciable spatial anisotropy. With a parton scattering cross section of about 10 mb, recent data on hadron isotropic flows from Au + Au collisions at $\sqrt{s} = 200$ AGeV can be approximately reproduced. Our results further show that the v_4 is a more sensitive probe of the initial partonic dynamics in these collisions than the v_2 , and that higher-order parton anisotropic flows are nonnegligible and satisfy the scaling relation $v_{n,q}(p_T) \sim v_{2,q}^{n/2}(p_T)$. Using the quark coalescence model, we then show that the parton scaling relation leads naturally to the observed similar scaling relation among hadron anisotropic flows. Studies of higher-order anisotropic flows in relativistic heavy ion collisions are thus expected to provide useful information on the collision dynamics and the properties of the hot dense matter during the initial stage.

Acknowledgments

We thank Vincenzo Greco, Peter Kolb and Ralf Rapp as well as Art Poskanzer and Nu Xu for useful discussions. This paper was based on work supported by the U.S. National Science Foundation under Grant No. PHY-0098805 and the Welch Foundation under Grant No. A-1358. L.W.C. was also supported by the National Natural Science Foundation of China under Grant No. 10105008.

[1] W. Reisdorf and H. G. Ritter, Ann. Rev. Nucl. Part. Sci. **47**, 663 (1997).
[2] J. Barrette et al. [E877 Collaboration], Phys. Rev. Lett. **73**, 2532 (1994).
[3] H. Appelshauser et al. [NA49 Collaboration], Phys. Rev. Lett. **80**, 4136 (1998).
[4] J.Y. Ollitrault, Phys. Rev. D **46**, 229 (1992).
[5] H. Sorge, Phys. Lett. **B402**, 251 (1997); Phys. Rev. Lett. **78**, 2309 (1997); Phys. Rev. Lett. **82**, 2048 (1999).
[6] P. Danielewicz, R. A. Lacey, P. B. Gossiaux, C. Pinkenburg, P. Chung, J. M. Alexander and R. L. McGrath, Phys. Rev. Lett. **81**, 2438 (1998).
[7] B. Zhang, M. Gyulassy and C. M. Ko, Phys. Lett. **B455**, 45 (1999).
[8] Y. Zheng, C. M. Ko, B. A. Li and B. Zhang, Phys. Rev. Lett. **83**, 2534 (1999).
[9] S. A. Voloshin, Nucl. Phys. **A715**, 379c (2003).
[10] P.F. Kolb, J. Sollfrank, and U. Heinz, Phys. Lett. **B459**,

667 (1999)

[11] D. Teaney and E.V. Shuryak, Phys. Rev. Lett. **83**, 4951 (1999);

[12] P.F. Kolb, J. Sollfrank, and U. Heinz, Phys. Rev. C **62**, 054909 (2000).

[13] P. F. Kolb, Phys. Rev. C **68**, 031902 (R) (2003) [nucl-th/0306081].

[14] J. Adams et al. [STAR Collaboration], [nucl-ex/0310029].

[15] B. Zhang, C. M. Ko, B. A. Li and Z. W. Lin, Phys. Rev. C **61**, 067901 (2000).

[16] Z. W. Lin, S. Pal, C. M. Ko, B. A. Li, and B. Zhang, Phys. Rev. C **64**, 011902 (2001); Nucl. Phys. **A698**, 375 (2002).

[17] Z. W. Lin and C. M. Ko, Phys. Rev. C **65**, 034904 (2002).

[18] Z. W. Lin, C. M. Ko and S. Pal, Phys. Rev. Lett. **89**, 152301 (2002).

[19] C.M. Ko, Z.W. Lin, and S. Pal, Heavy Ion Phys. 17, 219 (2003).

[20] X. N. Wang and M. Gyulassy, Phys. Rev. D **44**, 3501 (1991).

[21] B. Zhang, Comput. Phys. Commun. **109**, 193 (1998).

[22] T. Sjostrand, Comput. Phys. Commun. **82**, 74 (1994).

[23] B. A. Li and C. M. Ko, Phys. Rev. C **52**, 2037 (1995); B.A. Li, A.T. Sustich, B. Zhang, and C.M. Ko, Int. Jour. Phys. E **10**, 267-352 (2001).

[24] B. Zhang, C. M. Ko, B. A. Li, Z. W. Lin, and B. H. Sa, Phys. Rev. C **62**, 054905 (2000); B. Zhang, C. M. Ko, B. A. Li, Z. W. Lin, and S. Pal, *ibid.* **65**, 054909 (2002).

[25] S. Pal, C. M. Ko, and Z. W. Lin, Nucl. Phys. A730, 143 (2004).

[26] D. Kharzeev and M. Nardi, Phys. Lett. **B507**, 121 (2001).

[27] K. H. Ackermann et al., STAR Collaboration, Phys. Rev. Lett. **86**, 402 (2001).

[28] C. Adler et al., STAR Collaboration, Phys. Rev. Lett. **87**, 082301 (2001).

[29] Z. W. Lin and C. M. Ko, J. Phys. G 30 S263 (2004).

[30] A. M. Poskanzer and S. A. Voloshin, Phys. Rev. C **58**, 1671 (1998).

[31] P. Kolb, Talk at the RIKEN-BNL Workshop on Collective Flow and QGP Properties, Brookhaven National Laboratory, November 17-20, 2003, <http://tonic.physics.sunysb.edu/flow03> and to be published.

[32] D. Molnar and S. A. Voloshin, Phys. Rev. Lett. **91**, 092301 (2003).

[33] T.S. Biró et al., Phys. Lett. **B347**, 6 (1995); *ibid.* **472**, 243 (2002); Phys. Rev. C **59**, 1574 (1999); P. Csizmadia and P. Lévai, Phys. Rev. C **61**, 031903 (2000).

[34] V. Greco, C.M. Ko, and P. Lévai, Phys. Rev. Lett. **90**, 202302 (2003); Phys. Rev. C **68**, 034904 (2003).

[35] R.C. Hwa and C.B. Yang, Phys. Rev. C **67**, 034902 (2003); 064902 (2003).

[36] R.J. Fries, B. Müller, C. Nonaka, and S.A. Bass, Phys. Rev. Lett. **90**, 202303 (2003); Phys. Rev. C **68**, 044902 (2003).